An *In Situ* Infrared Study of CO_2 Reduction catalysed by Rhenium Tricarbonyl Bipyridyl Derivatives

Paul Christensen,[a] Andrew Hamnett,*[,a] Andrew V. G. Muir[a] and John A. Timney[b]
[a] *Department of Chemistry, Bedson Building, The University, Newcastle upon Tyne, NE1 7RU, UK*
[b] *Science Section, North Tyneside College, Wallsend NE28 9NJ, UK*

The electrochemical reduction of CO_2 by derivatives of rhenium carbonyl bipyridyl at carbon cathodes in acetonitrile solution is shown to take place by different routes depending on the concentration of water in the system. In the absence of water and CO_2, reduction of *fac*-[Re(dmbipy)$(CO)_3$Cl] (dmbipy = 4,4'-dimethyl-2,2'-bipyridyl) leads first to *fac*-[Re(dmbipy$^{\bullet-}$)$(CO)_3$Cl] followed by elimination of Cl^- and partial dimerisation of the resultant five-co-ordinate species to give both *fac*-[Re(dmbipy)$(CO)_3$] and [{Re(dmbipy)$(CO)_3$}$_2$]. Further reduction gives rise to *fac*-[Re(dmbipy$^{\bullet-}$)$(CO)_3$], which is the final product. Cathodic reduction of [Re(dmbipy)$(CO)_3$Cl] in the presence of CO_2 and absence of water leads to direct attack of CO_2 on *fac*-[Re(dmbipy$^{\bullet-}$)$(CO)_3$Cl] to give [Re(dmbipy)$(CO)_3(CO_2H)$] **E**, which can undergo further reduction to give [Re(dmbipy$^{\bullet-}$)$(CO)_2(CO_2H)$]. By contrast, in the presence of H_2O, the complex **E** can be protonated to yield [Re(dmbipy)$(CO)_3(CO_2H_2)$]$^+$ which is attacked by acetonitrile to yield [Re(dmbipy)$(CO)_3$(MeCN)]$^+$ and CO, this latter complex being identified unambiguously by comparison with the species formed in the *oxidation* of the original rhenium complex.

The development of low-overpotential methods for the electroreduction of CO_2 would have profound consequences for the economics of C_1 chemistry. At the moment, CO_2 has relatively little value as an end product of fossil-fuel combustion, even though the environmental disadvantages associated with its continued emission in large quantities into the atmosphere have been well documented.[1] The reasons for this are both thermodynamic and kinetic: the free energy of formation, $\Delta G_f^\circ = -394$ kJ mol^{-1}, a very negative value suggesting that rather high-energy reductants, such as H_2 are necessary for reduction to be possible. Electrochemically, reduction of CO_2 to CH_3OH takes place at an E° value of -0.38 V at pH 7, very close to the value for H_2 evolution at this pH. However, although this value is not by itself excessive, attempts to reduce CO_2 electrolytically normally require electrode potentials far negative of this value. The main origin of this kinetic barrier is the large gap between the lowest unoccupied (LUMO) and highest occupied molecular orbital (HOMO) in CO_2, and the E° value for the CO_2–CO_2^- redox couple has been estimated to be -2.21 V *vs.* the saturated calomel electrode (SCE).[2] Although the reduction process will certainly be facilitated by some stabilisation of the CO_2^- species, this kinetic barrier has been a major problem in the development of facile electroreduction processes, and a large effort is now being made worldwide to find more effective electrocatalysts.

The uncatalysed reduction pathways for CO_2 reduction have been enumerated by Saveant and co-workers,[3] and are summarised in Scheme 1. It is evident that the main stable reduction products on this scheme are CO, $C_2O_4^{2-}$ for HCO_2^-. In aqueous solution, the latter is predominant, with the evidence for CO_2^- formation being, at best, indirect,[4–6] and recent *in situ* Fourier transform infrared spectroscopy (FTIR) studies identifying a triply-bonded intermediate, Pt_3CO for CO_2 reduction on platinum.[7]

Most fundamental investigations in aqueous solution have been carried out at platinum and mercury electrodes, the latter having the immense advantage that hydrogen evolution is kinetically suppressed. However, other metals show a more enhanced electroactivity, though often with rather low current efficiency. Thus, tin and indium both have lower overvoltages,[8] and ruthenium appears to reduce CO_2 to CH_4 at potentials as low as -0.6 V *vs.* SCE[9,10] with a mechanism showing similarities to the Fischer–Tropsch process.[11] Copper electrodes also favour methane production, though at higher overpotentials.[12,13]

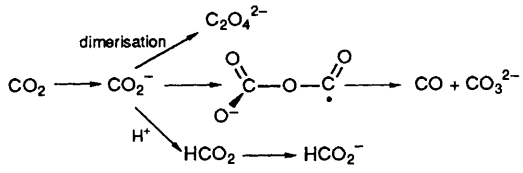

Scheme 1 Uncatalysed electrochemical pathway for reduction of CO_2

In aprotic solvents, the two upper routes in Scheme 1 predominate, this behaviour arising from the fact that the CO_2^- species is *radical*-like at the carbon but highly *basic* at the oxygens.[14] For reduction of CO_2 on mercury in dimethylformamide (dmf), dimerisation of the CO_2^- radical to give oxalate is favoured[15] whereas reduction on gold in acetonitrile yields CO and CO_3^{2-}.[16] In the latter case, as water is added, the CO is replaced by HCO_2^-.

It is clear from the above that electrocatalysis is likely to be needed if the overpotential for CO_2 reduction is to be lowered. Co-ordination of CO_2 to transition metals has recently been reviewed,[17] though it is clear that the co-ordination chemistry of CO_2 is still poorly understood. However, it is well known that CO_2 will insert into metal–ligand bonds, and these reactions have been well studied. Insertion into [M]–H bonds can proceed *via* two possible pathways to give either a metal–formate complex of the form [M]–O–CH=O[18] or a metal carboxylate (hydroxycarbonyl) of the form [M]–CO_2H, with the former being kinetically favoured.[19] In addition, attack of CO_2 at already co-ordinated ligands may offer a catalytic route.[20]

Exploitation of this type of complex in electrocatalytic reduction of CO_2 is still comparatively rare, and recent reviews have identified only a comparatively small number of systems.[21,22] Metal phthalocyanines adsorbed on carbon have been known[23] for some years to reduce CO_2, with the cobalt derivative being the most active. However, there is still considerable controversy over the distribution of products,[24,25]

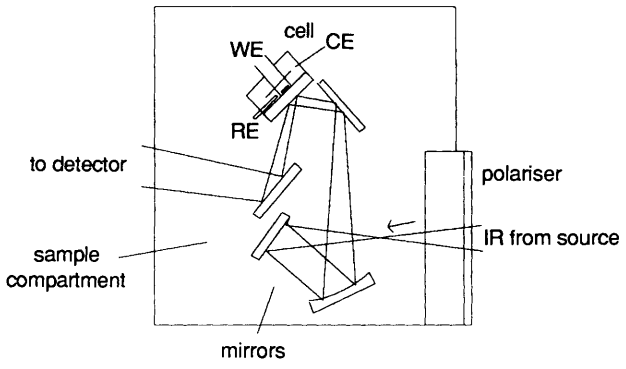

Fig. 1 Arrangement of the cell inside the FTIR spectrometer; RE = reference electrode, WE = working electrode, CE = counter electrode

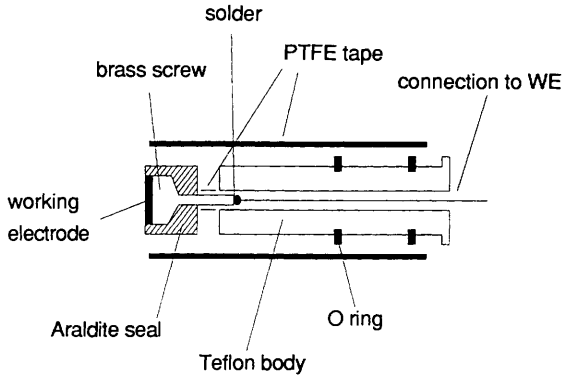

Fig. 2 The working electrode used for *in situ* FTIR studies

with oxalic,[23] glycolic[23] and formic[24] acids being reported as well as CO.[25] A mechanistic study with *in situ* FTIR spectroscopy suggested that CO_2 insertion into a Co–H bond was the primary route,[26] in agreement with earlier suggestions.[25,27,28] Other macrocycles have also been investigated, with [Ni(cyclam)Cl_2] (cyclam = 1,4,8,11-tetraazacyclotetradecane) being remarkably selective for CO production when adsorbed on mercury.[29]

Organometallic complexes have also been investigated as possible electrocatalysts. Complexes containing carbonyl and 2,2′-bipyridyl (bipy) ligands have been studied as the latter offers π^* orbitals close in energy to the antibonding d orbitals of the later transition elements, so allowing the complex to act as an electron sink. Thus, [Re(bipy)$(CO)_3Cl$] can convert CO_2 to CO with 95% current efficiency at −1.5 V in mixed protic/aprotic media[30] without appreciable loss of activity over 300 cycles,[31] though the mechanism is not fully understood.[30–33] Related systems include the complexes [M$(bipy)_2$-$(CO)R]^+$ (M = Os or Ru) where associative attack by CO_2 on the direduced complex leads to either CO or, in the presence of water, HCO_2H.[34] Certain phosphine complexes have also been found to show some activity.[35]

The mechanism of the mediated electrochemical reduction of CO_2 by [Re(bipy)$(CO)_3Cl$] and related complexes has been the subject of considerable study, both in solution and as polymer-bound species, and details of the suggested mechanisms are given below. All the mechanisms postulate a carboxylato species formed by attack of CO_2 on either a one- or two-electron reduction product of the starting complex. Such species should lend themselves to characterisation by infrared, and in order to investigate further the mechanism of the reaction between reduced organometallic complexes and CO_2, we have carried out an *in situ* FTIR investigation of the electrochemistry of [Re(dmbipy)$(CO)_3Cl$] (dmbipy = 4,4′-dimethyl-2,2′-bipyridyl) in the presence and absence of CO_2 and with varying concentrations of water in acetonitrile. The results point to rather different mechanisms in protic and aprotic media and indicate the power of the technique in identifying the primary routes.

Experimental

The complex [Re$(CO)_3$(dmbipy)Cl] was prepared according to the method of Wrighton and Abel;[36] [Re$(CO)_5Cl$] (Aldrich, used as received) and 4,4′-dimethyl-2,2′-bipyridyl (Aldrich, as received) were refluxed under nitrogen in hexane for 5 h and the resulting yellow solid filtered off, washed with hexane and dried *in vacuo* over silica gel. Found (calc.): C, 35.85 (36.75); H, 2.35 (2.45); Cl, 7.3 (7.25); N, 5.5 (5.70%). IR, KBr disc, 2021, 1925 and 1885 cm^{-1} (C≡O stretch). UV (in CH_2Cl_2): λ 373, 288 and 232 nm. The complex prepared in this way is reported to be in the *fac* form,[36] though the IR data cannot by itself distinguish between this and the *mer* form purely on symmetry grounds, since the symmetry of both complexes is sufficiently low for coupling to make all three bands visible in both cases. The IR spectra however are not consistent with a mixture of isomers.

Tetraethylammonium tetrafluoroborate was recrystallised from ethanol and tetrabutylammonium chloride was recrystallised under N_2 from acetone by addition of diethyl ether. Acetonitrile was distilled from calcium hydride under nitrogen and swiftly transferred to the electrochemical cell for purging with either CO_2 or N_2.

The FTIR spectrometer used was a Digilab Qualimatic QS100 (QC rev 2.53) with a wide-band mercury cadmium telluride (MCT) detector cooled by liquid nitrogen, and a Globar source. Potential control at the working electrode was achieved by a dedicated galvanostat/potentiostat card (Oxsys Micros) controlled by a 68000-based microprocessor.[37] The cell was constructed from 3 cm o.d. glass with an IR-transmitting plane window (CaF_2 from Spectra-Tech) glued to the cell using Araldite Rapid adhesive.* The cell volume was *ca.* 25 cm^3. A Spectra-Tech Series 500 variable-angle specular reflectance attachment allowed measurements to be carried out at angles of incidence between 30 and 80°: usually the angle was 55°, but the optimum angle was found for each particular set-up of electrolyte and window. A KRS-5 wire-grid polariser in front of the detector removes the superfluous information contained in the s-polarised light and helps to improve the signal-to-noise ratio. The arrangement of the cell inside the sample compartment is shown in Fig. 1. The working electrode, a glassy carbon disc of diameter 7 mm, is secured by silver araldite to a 3 mm brass screw head and sealed into a Teflon barrel: two 'Viton' 'O' rings provide a seal against the cell which is reinforced by Teflon tape as shown in Fig. 2. The working electrode can then be adjusted to a position arbitrarily close to the CaF_2 window, thus defining a thin layer within which the electrochemistry can be controlled and IR spectra simultaneously obtained. This thin-layer geometry also prevents significant interaction with any species formed at the counter electrode.

The IR spectra are presented as $\Delta R/R$, where $\Delta R = R(E_2) - R(E_1)$, R is the reflected intensity and E_1, E_2 are the potentials at which the spectra are measured. The normal procedure is to choose one potential at which a *reference* spectrum is measured, and to take spectra at successive potentials, E_i. It follows that positive peaks in the $\Delta R/R$ spectra represent absorptions from species that *decrease* in concentration in the thin layer on taking the potential from the reference value to the working value, and, conversely, negative peaks represent species that *gain* in concentration in the thin layer.

The glassy-carbon electrode was polished with alumina of varying particle size, down to 0.03 μm. The reflectivity of the electrode can be readily checked by using the 'align' function of the spectrometer, which returns the peak-to-peak voltage at

* A plane window was used since the off-centre parabolic mirrors within the spectrometer did not collimate the beam well enough to allow the use of prismatic windows.

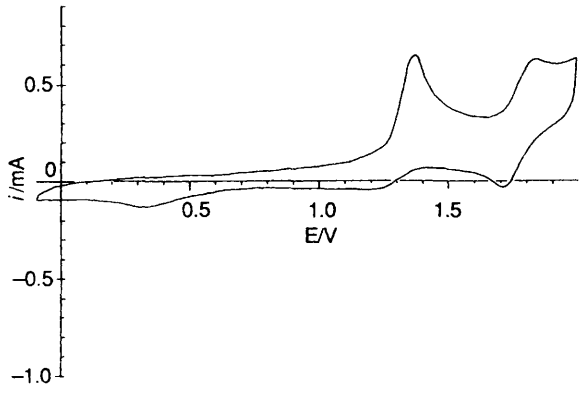

Fig. 3 Cyclic voltammogram of a glassy carbon electrode immersed in nitrogen-saturated acetonitrile containing NEt_4BF_4 (0.2 mol dm^{-3}) and [Re(dmbipy)$(CO)_3Cl$] (5 × 10^{-3} mol dm^{-3}). Scan rate: 100 mV s^{-1}

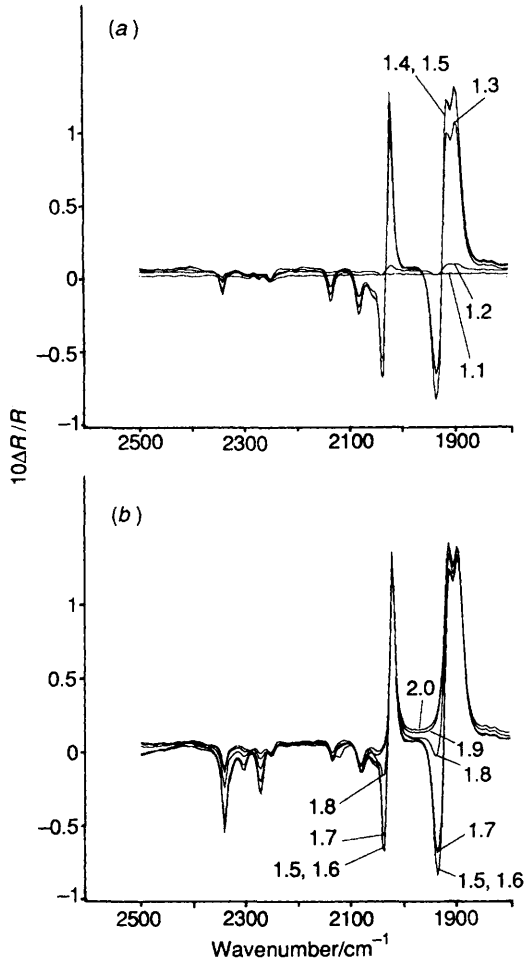

Fig. 4 FTIR spectra (8 cm^{-1} resolution, 69 scans, 3 min per spectrum) collected from the glassy carbon electrode immersed in the solution of Fig. 3. Spectra were collected at: (*a*) 1.1, 1.2, 1.3, 1.4 and 1.5 V; (*b*) 1.5, 1.6, 1.7, 1.8, 1.9 and 2.0 V. All spectra were normalised to the reference spectrum taken at the base potential of 1.0 V

the detector: measuring the decrease in detector voltage output when the electrode is pulled back from the window shows the amount of signal which is due to reflection from the electrode alone. The reference electrode used was a Radiometer Copenhagen K4112 saturated calomel electrode placed as close as possible to the working electrode and secured in an SQ 13 housing. The counter electrode is a platinum wire circling the working electrode. The spectrometer is mounted on an Ealing Instruments air table to minimise the effect of low-frequency vibrations upon the mirror travel, and the sample compartment purged by nitrogen from a boil-off supply to eliminate fluctuations in CO_2 and water vapour: the N_2 supply can also be used to drive the solution into the cell without the need to open the sample compartment or move the cell in its mounting. Fans used to cool the electronics are wall-mounted to minimise vibration.

The carbonyl stretching frequencies of the complexes formed during electrochemical oxidation and reduction of the parent compound have been analysed using energy-factored force constants,[38] and the method itself is reviewed in detail in the Appendix to this paper. The method used is remarkably accurate for neutral mononuclear transition-metal complexes, with a root mean square (r.m.s.) error of ≈ 5 cm^{-1}. The method is less accurate for anionic or cationic complexes in polar solvents, but generally is capable of predicting ν(CO) with an r.m.s. error of ≈ 8 cm^{-1}.

Results and Discussion

(*a*) *Anodic Behaviour of* [Re(dmbipy)$(CO)_3Cl$].—There is some controversy over the redox behaviour of [Re(dmbipy)-$(CO)_3Cl$],[32,39,40] notwithstanding the fact that the chemistry is somewhat simpler than the cathodic reduction. The cyclic voltammogram of [Re(dmbipy)$(CO)_3Cl$] in Fig. 3 shows two anodic waves, with peaks at +1.4 and +1.8 V *vs.* SCE in deoxygenated acetonitrile solution, and as Fig. 4 shows, each of these electrochemical processes is reflected in changes in the IR spectra.

At around +1.2 V sharp changes in absorption in the carbonyl stretching region begin, which are *bipolar*. The carbonyl absorption frequency has shifted to *higher* wavenumber for the band at 2023 cm^{-1}, which shifts to 2039 cm^{-1}, the band at 1906 which shifts to a poorly resolved shoulder at 1948 cm^{-1} and the 1893 cm^{-1} band which moves to 1935 cm^{-1}. This is consistent with oxidation of Re^{I} to Re^{II}: as the electron density on the metal decreases, the amount of $d_\pi(Re) \longrightarrow p_{\pi^*}(CO)$ back donation decreases, the C–O bond is strengthened as the antibonding orbital population falls, and the carbonyl stretching frequency rises.[41] Further changes are apparent as the potential is stepped towards 2.0 V, including the appearance of a peak at 2340 cm^{-1}: this is due to CO_2 produced by the oxidation of CO in the complex in the presence of adventitious water in the system: $CO + H_2O \longrightarrow CO_2 + 2e^- + 2H^+$. At 2273 cm^{-1} there is a gain of absorbance which can be attributed to a modified C≡N stretch of acetonitrile. The absorbance of the acetonitrile is shifted from its 'free' value of 2250 cm^{-1} to 2273 cm^{-1}, lending support to the idea that it undergoes co-ordination; the lone pair on the sp-hybridised nitrogen of MeCN is slightly antibonding and so donation to a (positive) metal centre will increase the C≡N stretching frequency.[42]

Two possibilities have been suggested for the fate of [Re(dmbipy)$(CO)_3Cl$] on oxidation: the first is loss of chloride followed by co-ordination of acetonitrile,[38,40] the other is loss of a carbonyl prior to solvent co-ordination,[32] although in this latter case the workers concerned did not detect any CO. At first sight, the appearance of a band at 2143 cm^{-1} might be regarded as unambiguous proof that CO is lost, since it is very close to the position expected for free CO. However, the fact that *three* absorptions are seen for the first oxidation product in the carbonyl region rules out carbonyl loss from the complex, and loss of chloride ion appears to be taking place. This is strongly supported by our calculations: the published ligand effect constants for acetonitrile are given elsewhere,[40] and we predict that *fac*-[Re(dmbipy)$(CO)_3(MeCN)]^+$ will have ν(CO) absorptions at 2043, 1959 and 1944 cm^{-1}, in reasonably good agreement with those observed. Other possibilities were tried to account for the three observed ν(CO) absorptions, but none was successful; in particular, the predicted frequencies of

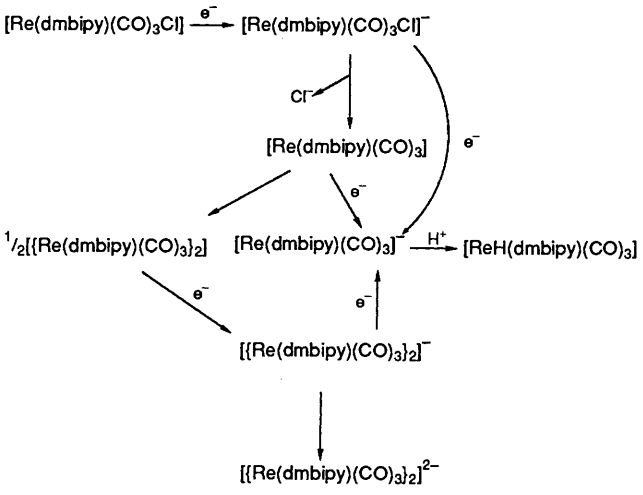

Scheme 2 Various courses proposed for the cathodic behaviour of [Re(dmbipy)(CO)$_3$Cl] under nitrogen

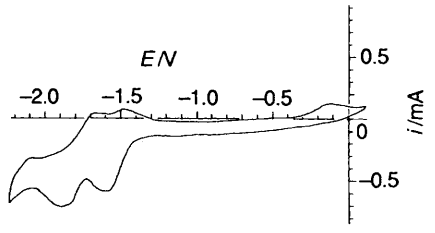

Fig. 5 Cyclic voltammogram of a glassy carbon electrode immersed in nitrogen-saturated acetonitrile containing NEt_4BF_4 (0.2 mol dm^{-3}) and [Re(dmbipy)(CO)$_3$Cl] (5 × 10^{-3} mol dm^{-3}). Scan rate: 100 mV s^{-1}

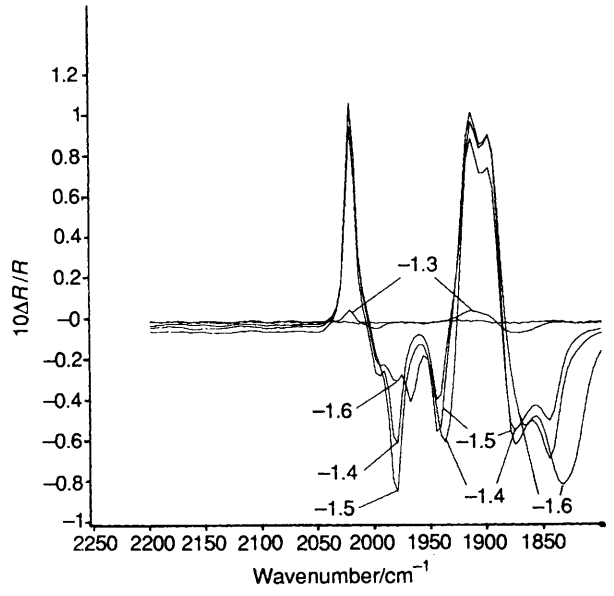

Fig. 6 FTIR spectra collected from a glassy carbon electrode immersed in the solution of Fig. 3. Spectra were collected at −1.2 to −1.6 V in 100 mV steps and normalised to the reference spectrum collected at −1.0 V

[Re(dmbipy)(CO)$_3$Cl]$^+$ are at 2089, 2007 and 2043 cm^{-1}, very much higher than those observed.

It therefore appears that oxidation leads to a 17-electron compound which immediately loses chlorine and gains a co-ordinated acetonitrile molecule to regain an 18-electron configuration [equation (1)].

$$[Re(dmbipy)(CO)_3Cl] \longrightarrow [Re(dmbipy)(CO)_3Cl]^+ + e^- \longrightarrow [Re(dmbipy)(CO)_3(MeCN)]^+ + \tfrac{1}{2}Cl_2 \quad (1)$$

There is, in addition to the bands already assigned, clear evidence of bands at 2143 and 2080 cm^{-1}, which appear almost as soon as the bands at lower wavenumber, and which are not associated with the further electrochemical process at 1.8 V. It would appear that this observation results from a minor pathway for the first oxidation process, and the molecule that best fits the spectroscopic data is one in which the dmbipy ligand has 'slipped' and is behaving as an η^6-arene ligand:

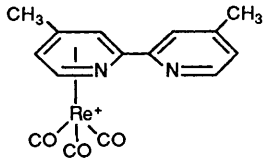

The ligand effect constant for the η^6-dmbipy ligand is not known, but if it is fitted to frequencies at 2143 and 2080 cm^{-1}, the calculated force constants (k_{CO} = 1783 N m^{-1}; k_i = 35 N m^{-1}) are in line with those expected for this type of molecule. It is of interest to note that calculations for *fac*-[Re(CO)$_3$(dmbipy)(MeCN)]$^{2+}$ lead to predicted frequencies at 2147, 2079 and 2065 cm^{-1}. If the latter two were unresolved, this would also correspond to the observed spectrum, but would be inconsistent with the electrochemical data, which only show a second oxidation process above 1.8 V, whereas the 2080 cm^{-1} feature is seen at much lower potentials. It is clear that the overall oxidation process is irreversible; the loss of chloride leaves a rhenium(I) complex which, as we will see below, is not reduced until rather negative potentials.

In the second oxidation region, the C≡O stretches at 2040 and 1930 cm^{-1} are lost as shown in Fig. 4(*b*), whilst there is a marked increase in the CO_2 peak, and in the peak due to co-ordinated acetonitrile. Furthermore, the complex is being degraded, since on stepping back down (towards 0 V) the bands do not re-appear and therefore the behaviour is not reversible. There are no obvious large *gains* in the carbonyl region, which suggests that the product has no CO groups bonded to the metal.

In conclusion, then, the oxidation of [Re(dmbipy)(CO)$_3$Cl] produces chlorine and the rhenium(II) complex *fac*-[Re(dmbipy)(CO)$_3$(MeCN)]$^+$, characterised by strong absorbances at 2039, 1948 and 1935 cm^{-1}. A subsidiary pathway involves loss of Cl and isomerisation of the dmbipy ligand rather than co-ordination of acetonitrile, to give [Re(η^6-dmbipy)(CO)$_3$]$^+$. Further oxidation leads to destruction of the complex to an unknown form, which appears not to be a metal carbonyl.

(*b*) *Cathodic Behaviour of* [Re(dmbipy)(CO)$_3$Cl] *under Nitrogen.*—The cathodic behaviour of [Re(dmbipy)(CO)$_3$Cl] has been the subject of some investigation, and the suggested reaction sequence is summarised[30,32,33] in Scheme 2. Some of the postulated species have been characterised previously, and the IR data are as follows; [{Re(dmbipy)(CO)$_3$}$_2$], ν(C≡O) at 2020, 1940 and 1860 cm^{-1} [30] although the higher-energy stretch has also been reported at 1975 cm^{-1},[40] and [ReH(dmbipy)(CO)$_3$], ν(C≡O) at 1993, 1905 and 1888 cm^{-1};[43] with ν(Re–H) at 2018 cm^{-1}.[43]

The cyclic voltammogram in Fig. 5 shows two cathodic waves and the FTIR spectra, resulting from stepping down the potential (*vs.* SCE) at the glassy carbon working electrode, are shown in Fig. 6. Large changes in the carbonyl stretching region are apparent, the most obvious difference from the anodic behaviour being that the bipolar shifts are to *lower* wavenumber, that is the carbonyl stretching frequencies are *decreased* as the metal becomes more electron rich and the extent of d_π(Re) ⟶ p_{π^*}(CO) donation increases. Initially, at −1.3 V, there are small loss and gain peaks that are very nearly symmetrical, with a gain at in the high-frequency region at *ca.* 1993 cm^{-1}, and in the low-frequency region at *ca.* 1875 cm^{-1}; these we associate with species **A**.

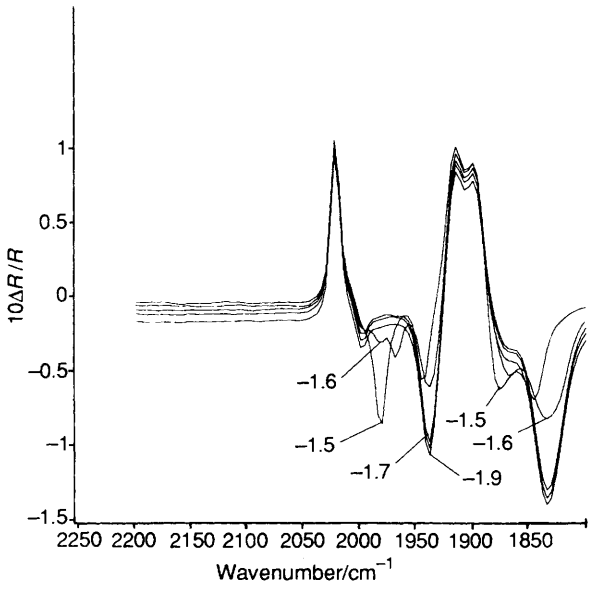

Fig. 7 FTIR spectra collected at −1.5 to −1.9 V in 100 mV steps and normalised to the reference spectrum collected at −1.0 V for the system described in Fig. 6

When the potential has reached −1.4 V the most intense gain in the high-frequency region is at 1979 cm^{-1}, with a second peak at 1943 cm^{-1} and new bands in the lower-energy carbonyl region are found at 1843 and 1876 cm^{-1}. This appears to be a composite of at least two species **B** and **C**. At −1.5 V, the only additional change is the further increase in all the peak intensities, with the final disappearance of the peak at 1993 cm^{-1} associated with the first species **A**. At −1.6 V, the spectrum changes substantially, with the higher frequency bands being replaced by ones at 1960 and 1930 cm^{-1}, whereas the lower frequency region becomes dominated by a band at 1830 cm^{-1} with a smaller band at 1865 cm^{-1}; this is associated with species **D**.

The effect of further reduction is shown in Fig. 7, in which the potential is taken down to −1.9 V. The dominant features seen in this region are at 1943 and 1828 cm^{-1}, the latter being broad. These absorptions are from the species formed at this cathodic limit, which we associate with species **E**.

Addition of one electron to $[Re(dmbipy)(CO)_3Cl]$ would produce the $19e^-$ $[Re(dmbipy)(CO)_3Cl]^-$, which is not expected to be stable if the electron were on the metal. Cabrera and Abruna[44] suggested that the product of reduction was the $Re^I(dmbipy^{\bullet -})$ species, and this is reasonable since Re^I will have the low-spin t_{2g}^6 configuration, and any extra electron on the metal would be in a very high lying orbital. Further evidence for the existence of the formally $19e^-$ anion comes from photosubstitution studies of $[Re(MeCN)(CO)_3(phen)]^+$[45] (phen = 1,10-phenanthroline), the photoinduced reduction of CO_2 by $[Re(CO)_3(bipy)Br]$,[46] and studies of the reduction chemistry of $[Re(CO)_3(bipy)(SnPh_3)]$ and related compounds.[47]

From the spectroscopic viewpoint, we would qualitatively expect the ligand effect constants for the dmbipy ligand to decrease on gain of an electron. Indeed, recent work by Glyn *et al.*[48] has shown this to be true, with the decrease in ε^{trans} being far greater than ε^{cis}. Thus, the species with ν(CO) at 1993 and 1875 cm^{-1} can reasonably be assigned to *fac*-$[Re(dmbipy^{\bullet -})(CO)_3Cl]$. The ligand effect constants for $(dmbipy^{\bullet -})$ calculated with this assumption are $\varepsilon[dmbipy^{\bullet -}]^{cis} = -34$ N m^{-1} and $\varepsilon[dmbipy^{\bullet -}]^{trans} = -67$ N m^{-1}, both of which are considerably lower than for dmbipy itself. The derived ligand effect constants are used to calculate ν(CO) frequencies for other complexes described here.

Cabrera and Abruna[44] further suggested that *fac*-$[Re(dmbipy^{\bullet -})(CO)_3Cl]$ underwent a slow chemical reaction, the loss of Cl^- to give the Re^0 compound $[Re(dmbipy)(CO)_3(MeCN)]$. If acetonitrile is chemically bonded to the Re, the formal oxidation state of the Re may be written as $Re^I(dmbipy^{\bullet -})$, since otherwise this complex would again be a 19 electron species. The infrared data do not corroborate this scheme: the initial gain of an absorbance at 1990 cm^{-1} is replaced by gain to lower wavenumber, at 1979 cm^{-1}, but spectroscopic calculations are *not* consistent with acetonitrile co-ordination. However, loss of Cl^- does seem a likely route, and for the d^7 complex *fac*-$[Re(dmbipy)(CO)_3]$ we predict ν(CO) absorbances at 1984, 1862 and 1849 cm^{-1}, in good agreement with three of the four frequencies associated with species **B** and **C** above. We thus assign the peaks at 1979, 1876 and 1843 cm^{-1} to species **B**, the five-co-ordinate *fac*-$[Re(dmbipy)(CO)_3]$.

This leaves the peak at 1943 cm^{-1} unassigned, and it would seem at least plausible that it should be associated with the reported peak of the dimer $[\{Re(dmbipy)(CO)_3\}_2]$[30,40] at 1940 cm^{-1}. If we accept the higher energy stretch of this dimer to lie at 1975 cm^{-1},[40] then both this and the lower peak might well lie under peaks already assigned to the five-co-ordinate monomer. It would seem highly likely, therefore, that species **C** is the dimer, even though only one peak, at 1943 cm^{-1}, can be unambiguously assigned, and that the monomer and dimer exist in equilibrium under the conditions of the experiment. It should be emphasised that the use of ligand effect constants is restricted to mononuclear complexes, and it is, therefore, not possible to check the plausibility of the assignments of the dimer spectrum.

At the most negative potentials, the gain of absorbance at 1943 and 1828 cm^{-1} is due almost certainly to the formation of the anion $[Re(dmbipy)(CO)_3]^-$ since this is expected to be the final reduction product at sufficiently negative potentials. However, spectroscopic calculations do *not* support assignment of the additional electron to the Re centre, to form a five-co-ordinate d^8 species; the bands predicted for such a species would be 1896, 1762 and 1750 cm^{-1}, far lower than those observed. By contrast, using the ligand effect constants calculated for $(dmbipy^{\bullet -})$, we predict that the ν(CO) frequencies of the *fac*-$[Re(dmbipy^{\bullet -})(CO)_3]$ species are at 1967, 1836 and 1821 cm^{-1}. The two low-frequency vibrations correspond well to the broad feature observed at 1828 cm^{-1}, and, although the difference between 1967 and 1943 cm^{-1} is rather large, a combination of uncertainty over the ligand effect constants for $(dmbipy^{\bullet -})$, and the known lower reliability of the calculations for charged species in polar solvents, makes the overall assignment of **D** to *fac*-$[Re(dmbipy^{\bullet -})(CO)_3]$ reasonable. There is a small gain at 1990 cm^{-1} at these more negative potentials as well: this may be due to some limited formation of the hydride by attack with adventitious water, since this has been identified as having a band at 1990 cm^{-1} by O'Toole *et al.*[40]

This analysis leaves us with the problem of species **D**, which appears most likely to be due to another dimeric species. In fact, the most likely assignment of **D** is to the $[(OC)_3(dmbipy)Re–Re(dmbipy^{\bullet -})(CO)_3]$ anion, though again our calculational method is unable to confirm this.

We can, therefore, tentatively assign all the species in Scheme 2 with the exception of the direduced dimer. If our assignment is correct, then our results are not consistent with the suggestion by Meyer and co-workers[33] that reduction of the dimer, at relatively positive potentials, can give the anion $[Re(dmbipy)(CO)_3]^-$, before its formation by the direct reduction of $[Re(dmbipy)(CO)_3]$. Our results rather support the idea that monomer and dimer exist in equilibrium at −1.4 to −1.5 V before further reduction takes place.

There is no evidence for a gain of free CO (2150 cm^{-1}) upon reduction of the complex (Scheme 2) in which Cl^- is lost instead.

To summarise the behaviour in the *absence* of CO_2, then, reduction of *fac*-$[Re(dmbipy)(CO)_3Cl]$ leads initially to *fac*-$[Re(dmbipy^{\bullet -})(CO)_3Cl]$, which has a high-energy C≡O stretch at 1993 cm^{-1}. This reacts by loss of chloride to give $[Re(dmbipy)(CO)_3]$, which exists in equilibrium with the dimer $[\{Re(dmbipy)(CO)_3\}_2]$. The higher energy CO stretch of this

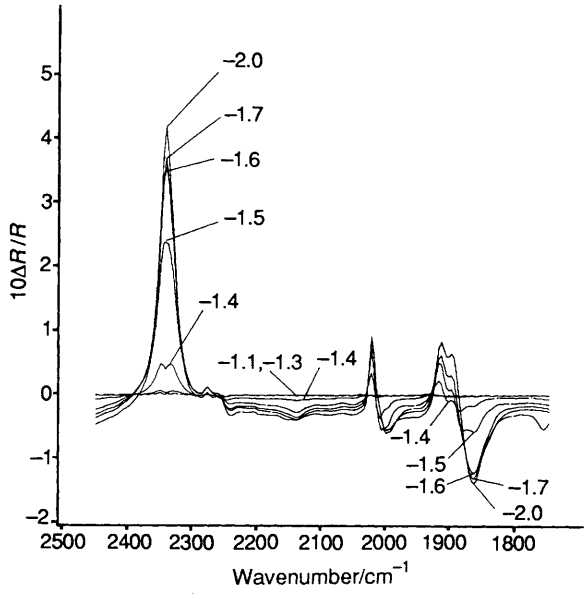

Fig. 8 FTIR spectra collected from the glassy carbon electrode immersed in CO_2-saturated acetonitrile containing NEt_4BF_4 (0.2 mol dm^{-3}) and [Re(dmbipy)$(CO)_3$Cl] (5×10^{-3} mol dm^{-3}). Spectra were collected at −1.1, −1.3, −1.4, −1.5, −1.6, −1.7 and −2.0 V and normalised to the spectrum collected at −1.0 V

species is at 1975 cm^{-1}, the lower frequency indicative of the oxidation state change of the metal despite the overall neutrality of the complex. There is also no evidence of any co-ordination of acetonitrile in the region near 2300 cm^{-1}. Further reduction to the anion *fac*-[Re(dmbipy$^{\bullet-}$)$(CO)_3$] is accompanied by a further shift of the CO stretches to lower wavenumber, as a consequence of the lower ligand effect constants of dmbipy$^{\bullet-}$.

(*c*) *Reduction of* [Re(dmbipy)$(CO)_3$Cl] *in the Presence of* CO_2.—When the negative-going scan is repeated in the presence of CO_2, the resulting FTIR spectra are rather different as shown in Fig. 8. The absorption at 2150 cm^{-1} due to the *gain* of CO, although weak, is clearly visible, as shown in Fig. 9(*a*). Taken in conjunction with the *loss* of CO_2 at 2342 cm^{-1} (this spectrum shows the loss is *initially of gas-phase* CO_2), it reveals the reduction of CO_2 by [Re(dmbipy)$(CO)_3$Cl], since formation of CO is not observed at all on platinum or glassy carbon at these potentials.

The amount of CO seen in the IR spectrum is small, an observation that results from both the comparatively low oscillator strength for absorption of IR by CO as compared to CO_2 (a factor of eight)[49] and the low solubility of CO in acetonitrile. In fact, the direct observation of CO as a reduction product in electrochemical CO_2 reduction is relatively unusual.[16]

The carbonyl stretching region, shown in more detail in Fig. 9(*b*) and 9(*c*), shows that *two* species form on reduction in the presence of CO_2, an initially formed complex, **E**, with peaks at 2010, 1902 and 1878 cm^{-1}, the middle one of these being to some extent obscured by the loss peak associated with the neutral form. At more negative potentials, a second complex, **F**, forms with peaks at 1997 and 1860 cm^{-1}, as shown in Fig. 9(*c*), with small amounts of a third species, **G**, at 1930 and 1828 cm^{-1} being seen at very negative potentials.

It has been suggested[30] that the dimer [{Re(dmbipy)$(CO)_3$}$_2$] does not form under CO_2, since [Re(dmbipy$^{\bullet-}$)$(CO)_3$Cl] will react faster with CO_2 than it would lose chloride and dimerise. The absence of peaks associated with either *fac*-[Re(dmbipy$^{\bullet-}$)-$(CO)_3$Cl], *fac*-[Re(dmbipy)$(CO)_3$] or its dimer strongly supports this view. Investigation of the spectral region below 1800 cm^{-1} reveals a sharp band at 1640 cm^{-1} that is not present in the absence of CO_2, as shown in Fig. 10. However, this can

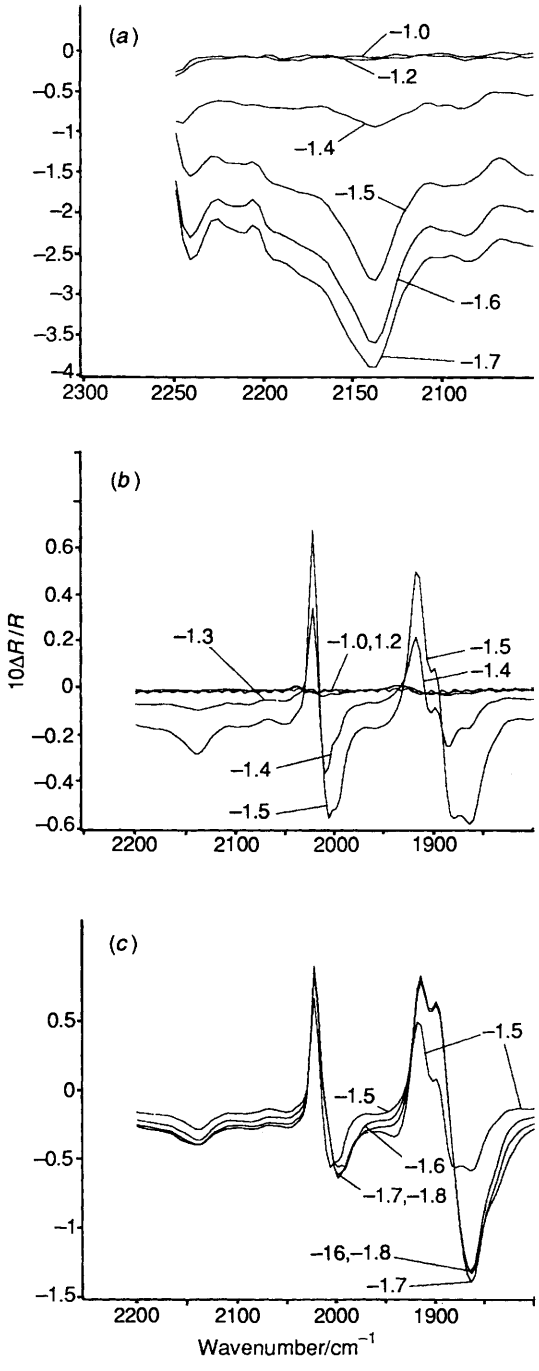

Fig. 9 (*a*) FTIR spectra in the region 2050–2250 cm^{-1} collected during the experiment of Fig. 8 at −1.0, −1.2, −1.4, −1.5, −1.6 and −1.7 V and normalised to the spectrum collected at −0.6 V; (*b*) corresponding spectra in the region 1800–2200 cm^{-1} at potentials −1.1 to −1.5 V in 100 mV steps, normalised to the spectrum at −1.0 V; (*c*) corresponding spectra in the region 1800–2200 cm^{-1} at potentials −1.5 to −1.8 V in 100 mV steps, normalised to the spectrum at −1.0 V

be assigned without difficulty to the carbonate ion in the form of an ion pair.[16] It should be emphasised, however, that the intensity of both the CO and carbonate bands is far smaller than that expected for complete conversion of the CO_2 to CO and CO_3^{2-},[16] suggesting that much of the CO_2 is held in the form of the two complexes, **E** and **F**. Unfortunately, the effect of the carbonate band is to obscure any metal formylate antisymmetric stretches which would also be expected in this region.[26]

Three mechanisms have been proposed for the reduction of CO_2. The first of these [equations (2a)–(2c), L = Cl^- (n = 0); L = MeCN (n = 1)] is a one-electron pathway.

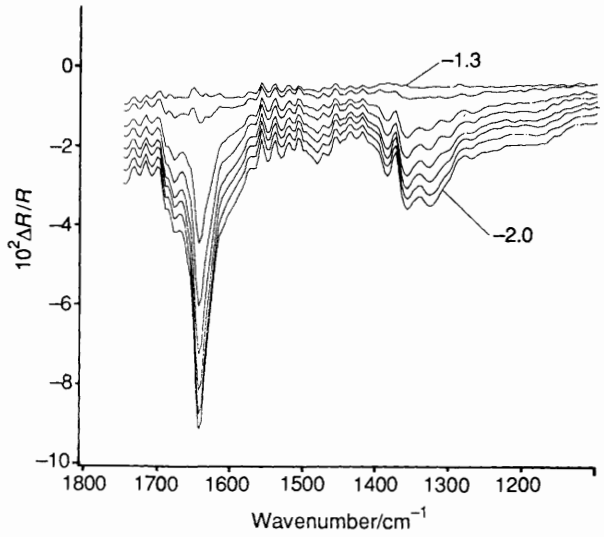

Fig. 10 FTIR spectra in the region 1100–1750 cm^{-1} collected during the experiment of Fig. 8 at potentials −1.3 to −2.0 V in steps of 100 mV and normalised to the spectrum collected at −1.0 V

$$[Re(dmbipy)(CO)_3Cl] + e^- \longrightarrow [Re(dmbipy)(CO)_3] + Cl^- \quad (2a)$$

$$[Re(dmbipy)(CO)_3] + CO_2 \longrightarrow [Re(dmbipy)(CO)_3(CO_2)] \quad (2b)$$

$$2[Re(dmbipy)(CO_3)(CO_2)] + 2L \longrightarrow 2[Re(dmbipy)(CO)_3L]^{n+} + CO + CO_3^{2-} \quad (2c)$$

In the second proposed mechanism[34] [equations (3a)–(3c),

$$[Re(dmbipy)(CO)_3] + e^- \longrightarrow [Re(dmbipy)(CO)_3]^- \quad (3a)$$

$$[Re(dmbipy)(CO)_3]^- + CO_2 \longrightarrow [Re(dmbipy)(CO)_3(CO_2)]^- \quad (3b)$$

$$[Re(dmbipy)(CO)_3(CO_2)]^- + CO_2 + L \longrightarrow [Re(dmbipy)(CO)_3L]^{n+} + CO + CO_3^{2-} \quad (3c)$$

L = Cl^- (n = 0), L = MeCN (n = 1)] a second molecule of CO_2 acts as an oxide ion acceptor, and this is a two-electron pathway.

The third mechanism[30] [equations (4a)–(4c)] is shown below.

$$[Re(dmbipy)(CO)_3Cl] + e^- \longrightarrow [Re(dmbipy)(CO)_2Cl]^- + CO \quad (4a)$$

$$[Re(dmbipy)(CO)_2Cl]^- + CO_2 + 2H^+ \longrightarrow [Re(dmbipy)(CO)_3Cl]^+ + H_2O \quad (4b)$$

$$[Re(dmbipy)(CO)_3Cl]^+ + e^- \longrightarrow [Re(dmbipy)(CO)_3Cl] \quad (4c)$$

Here reduction is thought to occur *via* a Re carboxylate; such species are known in the literature, *e.g.* [Re(η-C_5H_5)(CO)(*p*-$N_2C_6H_4R$)(CO_2H)] (R = alkyl) which can be prepared by the attack of OH^- upon a co-ordinated carbonyl group.[19] Once the carboxylate has formed, an oxide acceptor is then able to effect the protonation of the CO_2H group leading to loss of water and formation of co-ordinated CO. It has also been suggested[30] that the presence of excess chloride (for example) ensures the absence of a vacant co-ordination site on the metal and thus prevents formation of the dimer and/or hydride.

In the absence of a proton source, such as H_2O, the third mechanism can be discounted, particularly since it cannot account for the large production of CO_3^{2-} as well as CO. There is no evidence for the production of $[Re(dmbipy)(CO)_3]^-$ at the relatively positive potentials at which CO_2 is first reduced, and this would strongly suggest that the first, one-electron mechanism, is the most likely. In fact, since **A** is not seen, direct attack on the singly reduced species $[Re(dmbipy^{\bullet-})(CO)_3Cl]$ by CO_2 seems most likely. At more negative potentials, a more reduced species, **F**, is formed. Given the fact that this species also appears to contain co-ordinated CO_2, it is most likely that **E** is either $[Re^I(dmbipy)(CO)_3(CO_2^-)]$, or the protonated form $[Re^I(dmbipy)(CO)_3(CO_2H)]$ whose carbonyl stretches would be very close to those of $[Re^I(dmbipy)(CO)_3Cl]$. The possibility of the protonated form appearing cannot be ruled out since our system cannot completely exclude water, even under very carefully controlled experimental conditions.

Unambiguous assignment depends on reasonable values being available for the ligand effect constants of $-CO_2H$ and $-CO_2^-$: from the spectrum of *fac*-[Re(CO)$_3$(bipy)(CO_2H)], we obtain $\varepsilon[CO_2H]^{cis}$ = 137 N m^{-1} and $\varepsilon[CO_2H]^{trans}$ = 65 N m^{-1}, in line with values for similar ligands. Using these, we predict the ν(CO) frequencies for *fac*-[Re(dmbipy)(CO)$_3$(CO_2H)] to be at 2014, 1914 and 1864 cm^{-1}, in fair agreement with those observed for species **E**. Refining the fit gives, for $\varepsilon[CO_2H]^{cis}$ = 125 N m^{-1} and $\varepsilon[CO_2H]^{trans}$ = 90 N m^{-1}, best predicted values of 2012, 1905 and 1876 cm^{-1}. It is likely that this discrepancy in ligand effect constants is traceable, at least in part, to solvent effects.

There are two possibilities for species **F**. One is that **F** is a further reduced species; using the ligand effect constants for ($dmbipy^{\bullet-}$), we predict that the ν(CO) frequencies for *fac*-$[Re(dmbipy^{\bullet-})(CO)_3(CO_2H)]$ at 1992, 1867 and 1866 cm^{-1}, in good agreement with those observed. A second possibility is that **F** is the deprotonated form of **E**. Certainly this would be expected to cause shifts of the same order of magnitude between **E** and **F** as those observed, though the evolution of H_2 associated with the second of these on glassy carbon might be less favoured from the electrochemical point of view.

Finally, the complex seen at very negative potentials, which gives two bands at 1930 and 1823 cm^{-1}, could be *fac*-$[Re(dmbipy^{\bullet-})(CO)_3(CO_2H)]^-$. We predict that the ν(CO) bands for this molecular anion should occur at 1936, 1816 and 1815 cm^{-1}, in good agreement with the observed values.

The mechanism that emerges from these studies is then, in the absence of appreciable concentrations of proton donor given by equations (5a)–(5dii).

$$[Re(dmbipy)(CO)_3Cl] + e^- \longrightarrow [Re(dmbipy^{\bullet-})(CO)_3Cl] \quad (5a)$$

$$[Re(dmbipy^{\bullet-})(CO)_3Cl] + CO_2 \longrightarrow [Re(dmbipy)(CO)_3(CO_2)] + Cl^- \quad (5b)$$

$$[Re(dmbipy)(CO)_3(CO_2)] + e^- + H_2O \longrightarrow [Re(dmbipy)(CO)_3(CO_2H)] + OH^- \quad (5ci)$$

and

$$OH^- + CO_2 \longrightarrow CO_3^{2-} + H^+ \quad (5cii)$$

or

$$2[Re(dmbipy)(CO)_3(CO_2)] + 2Cl^- \longrightarrow 2[Re(dmbipy)(CO)_3Cl] + CO + CO_3^{2-} \quad (5ciii)$$

$$[Re(dmbipy)(CO)_3(CO_2H)] + e^- \longrightarrow [Re(dmbipy^{\bullet-})(CO)_3(CO_2H)] \quad (5di)$$

or

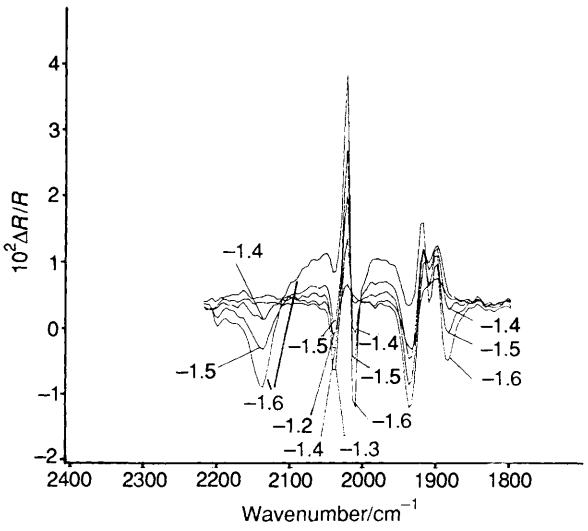

Fig. 11 FTIR spectra collected from the glassy carbon electrode immersed in CO_2-saturated acetonitrile–water (9:1) containing NBu_4Cl (0.2 mol dm^{-3}) and [Re(dmbipy)$(CO)_3Cl$] (5×10^{-3} mol dm^{-3}). The spectra were taken between −1.2 and −1.6 V in 100 mV steps and ratioed to the spectrum collected at −1.0 V

$$[Re(dmbipy)(CO)_3(CO_2H)] + e^- \longrightarrow [Re(dmbipy)(CO)_3(CO_2^-)] + \tfrac{1}{2}H_2 \quad (5dii)$$

In this mechanism, reaction (5b) is fast, ensuring that the stationary concentration of $[Re(dmbipy)(CO)_3Cl]^-$ remains low. Reaction (5ci) must also be fast, given the fact that we do not appear to detect the radical species, and the main evidence for step (5ciii) is the appearance of a weak CO band. Unfortunately, as indicated above, it has not proved possible to identify the expected carboxylato stretches near 1650 cm^{-1} owing to the presence of strong CO_3^{2-} bands.

The conditions used in the above experiment, namely nominally dry acetonitrile and a non-co-ordinating anion as the electrolyte (BF_4^- or PF_6^-), do not represent those reported to be most efficient for the reduction of CO_2.[44] When the experiment is repeated with NBu_4Cl as the supporting electrolyte, and in the presence of 10% water, which has been reported to be the optimum conditions,[31] the FTIR spectra under CO_2 are rather different as shown in Fig. 11.

Again, there are gains of absorbance to lower wavenumber of the unreduced complex carbonyl bands, the most prominent of which are at 2010, 1935 and 1873 cm^{-1}. However, the most remarkable feature of the spectra is the appearance of gains to *higher* wavenumber of the [Re(dmbipy)$(CO)_3Cl$] bands, at 2040 cm^{-1}. Additionally, the amount of CO formed (gain of absorbance at 2150 cm^{-1}) is much greater than in dry acetonitrile (with NEt_4BF_4 as electrolyte).

The shift of carbonyl bands to *higher* wavenumber upon *reduction* is at first surprising, given that the behaviour described above was the opposite, *i.e.* shifts to lower wavenumber. Now, the spectra imply the presence of either a rhenium(II) complex or a *cationic* complex of rhenium(I). A cationic complex is expected to have ν(C≡O) raised relative to the neutral or anionic complex, as shown in the Appendix. In fact, the spectrum of this complex closely resembles that of the complex formed on *anodic* oxidation in the absence of CO_2, which was assigned as $[Re(dmbipy)(CO)_3(MeCN)]^+$, a cationic complex of rhenium(I). This is seen by comparing Figs. 4 and 11. As we might also expect, there is now considerable structure evident also in the acetonitrile region, quite different from the situation in the absence of large amounts of water.

The oxidation state for rhenium in the cationic complex formed is +1, and, as indicated above, reduction of Re^I only takes place at relatively negative potentials. It can be seen from the figure that the maximum concentration of the $[Re(dmbipy)(CO)_3(MeCN)]^+$ complex is found at −1.3 V; below this, it rapidly disappears as further reduction takes place. It is clear, then, that a sustained turnover of CO_2 can only be achieved at potentials of −1.4 V or below, since only at these potentials can a complete cycle be obtained.

We may thus put forward the following mechanism [equations (6a)–(6e)] for CO_2 reduction by [Re(dmbipy)$(CO)_3Cl$] in the presence of water.

$$[Re(dmbipy)(CO)_3Cl] + e^- \longrightarrow [Re(dmbipy^{\bullet -})(CO)_3Cl] \quad (6a)$$

$$[Re(dmbipy^{\bullet -})(CO)_3Cl] + CO_2 \longrightarrow [Re(dmbipy)(CO)_3(CO_2)] + Cl^- \quad (6b)$$

$$[Re(dmbipy)(CO)_3(CO_2)] + e^- + H^+ \longrightarrow [Re(dmbipy)(CO)_3(CO_2H)] \quad (6c)$$

$$[Re(dmbipy)(CO)_3(CO_2H)] + MeCN + H^+ \longrightarrow [Re(dmbipy)(CO)_3(MeCN)]^+ + CO + H_2O \quad (6d)$$

$$[Re(dmbipy)(CO)_3(MeCN)]^+ + 2e^- \longrightarrow [Re(dmbipy^-)(CO)_3] \quad (6e)$$

Steps (6b) and (6c) are certainly fast, but step (6d) would appear to be sufficiently slow for the carboxylato complex to diffuse away from the electrode before CO formation takes place. One reason for this may be that reaction (6c) tends to denude the region near the electrode of protons, so slowing reaction (6d) down.

In support of this mechanism, there is no longer a peak at 1650 cm^{-1} due to carbonate; instead, there are peaks at 1690 and 1720 cm^{-1}. These spectra are somewhat different from the spectra found for the CO_3^{2-} in MeCN–H_2O,[16] and one at least may be associated with the carboxylato complex. Values for similar rhenium complexes in the literature are 1646 and 1584 cm^{-1} for [Re(η-C_5H_5)(CO)(*p*-$N_2C_6H_4R$)(CO_2^-)],[50] 1663 cm^{-1} for $[IrCl_2(CO_2H)(CO)(PMe_2Ph)_2]$,[51] and 1591 cm^{-1} for [Re(η-C_5H_5)(NO)$(PPh_3)(CO_2H)$];[52] although these are rather lower than the absorbances in the spectra above, the dramatic affect of solvent co-ordination on the position of the C=O stretch (in carbonate) has already been noted.[16]

Conclusion

The use of *in situ* FTIR has enabled us, for the first time, to follow the details of the reduction mechanism for CO_2 with an organometallic catalyst. We have been able unambiguously to assign most of the spectra with the use of a straightforward but reliable and robust method for the prediction and analysis of carbonyl spectra using ligand effect constants. Combining this technique with the electrochemical data has enabled us to eliminate a number of otherwise plausible routes and to identify the likely slowest steps.

Appendix

The Prediction and Analysis of ν(CO) *Spectra.*—Some time ago, one of us (J. A. T.) published a method that enabled the ν(CO) frequencies of mononuclear transition-metal carbonyls to be predicted with remarkable accuracy[36] using energy-factored force constants. For uncharged complexes in hydrocarbon solvents, the r.m.s. error in observed *vs.* calculated values is about 5 cm^{-1}. The method is less accurate for anionic or cationic complexes in polar solvents, but generally predicts ν(CO) frequencies with an r.m.s. error of around 8 cm^{-1}.

To predict ν(CO) frequencies we need to calculate CO-stretching force constants, k_{CO}, and CO–CO interaction constants, $k_{CO,CO}$. The stretching force constants are calculated from equation (A1) where k_d is the CO stretching force constant

$$k_{CO} = k_d + \Sigma\varepsilon[L]^\theta + 197Q \quad (A1)$$

of the metal monocarbonyl, M–CO, and the terms contained within the summation are ligand effect constants that are transferrable between metal centres; Q is the charge on the metal. The ligand effect constants that most concern us here are those which quantify the effect of adding a ligand *cis* or *trans* to a CO group (ε^{cis} and ε^{trans} respectively.

The interaction constants are calculated from appropriate linear equations of the form (A2), where A and B are constants

$$k_{CO,CO} = A - B(k_{CO} - 120Q) \quad (A2)$$

that depend on the C–M–C angle. For 'regular' angles (90, 109.5, 120 and 180°) the values of A and B are well known. If *fac*-[$Re(CO)_3$(bipy)X] and *fac*-[Re(dmbipy)$(CO)_3$X] complexes had C–M–C bond angles near 90°, we would expect three ν(CO) bands with approximately equal intensity. That this is not the case means that specific values of A and B need to be calculated for these complexes. We find that the energy-factored CO–CO interaction constants of a number of *fac*-[$Re(CO)_3$(L–L)X] complexes (L–L = bipy, dmbipy, diamines; X = Cl, Br) are related to the stretching force constants (k_{CO}) by equation (A3). Unless otherwise noted, this relationship is used to calculate CO–CO interaction constants in this paper.

$$k_{CO,CO} = 206 - 0.0956k_{CO} \quad (A3)$$

Most of the molecules identified in this work retain the *fac*-[$Re(CO)_3$(L–L)X] structure. We have used ligand effect constants and equation (A3) to calculate the four energy-factored force constants required for a *fac*-[$Re(CO)_3$(L–L)X] structure. These are: k_1 (k_{CO} for the CO group *trans* to X), k_2 (k_{CO} for the CO group *cis* to X), $k_{1,2}$ (interaction constant linking k_1 and k_2) and $k_{2,2}$ (interaction constant linking the k_2 CO groups). These energy-factored force constants are then used to calculate the symmetry force constants, $K(\Gamma)$, for the three ν(CO) modes of *fac*-[$Re(CO)_3$(L–L)X]: equations (A4) and (A5). Finally, symmetry force constants are related to the ν(CO) frequencies by equation (A6).

$$\begin{bmatrix} k_2 + k_{2,2} - K(a') & \sqrt{2}k_{1,2} \\ \sqrt{2}k_{1,2} & k_1 - K(a') \end{bmatrix} = 0 \quad (A4)$$

$$K(a'') = k_2 - k_{22} \quad (A5)$$

$$\nu(\Gamma) = 49.756\sqrt{K(\Gamma)} \quad (A6)$$

Acknowledgements

J. A. T. thanks the Leverhulme Trust for a grant, and A. V. G. M. thanks the SERC for a studentship. We would also like to acknowledge helpful advice from Dr. S. J. Higgins.

References

1 T. Augutsson and V. Ramanathan, *J. Atmos. Sci.*, 1977, **34**, 448.
2 E. Lamy, L. Nadjo and J. M. Saveant, *J. Electroanal. Chem., Interfacial Electrochem.*, 1977, **78**, 403.
3 J. C. Gressin, D. Michelet, L. Nadjo and J.-M. Saveant, *Nouv. J. Chim.*, 1979, **3**, 545.
4 Yu. Vassiliev, N. S. Bagotsky, N. V. Osetrova, O. A. Khazova and N. A. Mayorova, *J. Electroanal. Chem., Interfacial Electrochem.*, 1985, **189**, 271.
5 A. Bewick and D. J. Schiffrin, *Faraday Discuss. Chem. Soc.*, 1973, **56**, 112.
6 A. W. B. Aymler-Kelly, A. Bewick, P. R. Cantrill and A. M. Tuxford, *Faraday Discuss. Chem. Soc.*, 1973, **56**, 96.
7 B. Beden, A. Bewick, M. Razaq and J. Weber, *J. Electroanal. Chem., Interfacial Electrochem.*, 1982, **39**, 203.
8 S. Kapusta and N. Hackerman, *J. Electrochem. Soc.*, 1983, **130**, 607.
9 K. W. Frese and D. Cranfield, *J. Electrochem. Soc.*, 1983, **130**, 1772; 1984, **131**, 2518.
10 K. W. Frese and S. Leach, *J. Electrochem. Soc.*, 1985, **132**, 259.
11 D. P. Summers and K. W. Frese, *Langmuir*, 1988, **4**, 51.
12 R. L. Cook and A. F. Sammells, *J. Electrochem. Soc.*, 1987, **134**, 2375; 1988, **135**, 1471.
13 J. Kim, D. P. Summers and K. W. Frese, *J. Electroanal. Chem., Interfacial Electrochem.*, 1988, **245**, 223.
14 D. W. Ovenall and D. H. Whiffen, *Mol. Phys.*, 1961, **4**, 135.
15 C. Amatore and J. M. Saveant, *J. Am. Chem. Soc.*, 1981, **103**, 5021.
16 P. A. Christensen, A. Hamnett and A. V. G. Muir, *J. Electroanal. Chem., Interfacial Electrochem.*, 1990, **228**, 197.
17 J. A. Ibers, in *CO_2 as a Source of Carbon: Biochemical and Chemical Uses*, NATO ASI Series C, 1987, **206**, 55.
18 D. J. Darensbourg, C. G. Bauch and C. Ovalles, *ACS Symp. Ser.*, 1988, **363**, 26.
19 S. Sakati and K. Ohkubo, *Inorg. Chem*, 1989, **28**, 2583.
20 D. Walther, *Coord. Chem. Rev.*, 1987, **79**, 135.
21 J. P. Collin and J. P. Sauvage, *Coord. Chem. Rev.*, 1989, **93**, 245.
22 I. S. Kolomnikov and T. V. Lysyak, *Usp. Khim.*, 1990, **59**, 589.
23 S. Meshitsuka, M. Ichikawa and K. Tamaru, *J. Chem. Soc., Chem. Commun.*, 1974, 158.
24 S. Kapusta and N. Hackerman, *J. Electrochem. Soc.*, 1984, **131**, 1511.
25 C. M. Lieber and N. S. Lewis, *J. Am. Chem. Soc.*, 1984, **106**, 5033.
26 P. A. Christensen, A. Hamnett and A. V. G. Muir, *J. Electroanal. Chem., Interfacial Electrochem.*, 1986, **241**, 361.
27 H. Tanabe and K. Ohno, *Electrochim. Acta*, 1987, **34**, 1121.
28 K. Kusida, R. Ishihara, H. Yamaguchi and I. Izumi, *Electrochim. Acta*, 1986, **31**, 657.
29 M. Beley, J. P. Collin, R. Ruppert and J. P. Sauvage, *J. Am. Chem. Soc.*, 1986, **108**, 7461.
30 J. Hawecker, J.-M. Lehn and R. Ziessel, *Helv. Chim. Acta*, 1986, **69**, 1990.
31 J. Hawacker, J.-M. Lehn and R. Ziessel, *J. Chem. Soc., Chem. Commun.*, 1984, 328.
32 A. I. Breikss and H. D. Abruna, *J. Electroanal. Chem., Interfacial Electrochem.*, 1986, **201**, 347.
33 B. P. Sullivan, C. M. Bolinger, D. Conrad, W. J. Vining and T. J. Meyer, *J. Chem. Soc., Chem. Commun.*, 1985, 1414.
34 M. R. M. Bruce, E. Megehee, B. P. Sillivan, H. Thorp, T. R. O'Toole, A. Downard and T. J. Meyer, *Organometallics*, 1988, **7**, 238.
35 D. L. DuBois and A. Miedaner, *J. Am. Chem. Soc.*, 1987, **109**, 113.
36 E. W. Abel and G. Wilkinson, *J. Chem. Soc.*, 1959, 1501; M. S. Wrighton and D. L. Morse, *J. Am. Chem. Soc.*, 1974, **96**, 998.
37 P. A. Christensen, A. Hamnett and P. R. Trevellick, *J. Electroanal. Chem., Interfacial Electrochem.*, 1988, **242**, 23.
38 J. A. Timney, *Inorg. Chem.*, 1979, **18**, 2502.
39 S. Cosnier, A. Deronzier and J.-C. Moutet, *J. Electroanal. Chem., Interfacial Electrochem.*, 1986, **207**, 315.
40 T. R. O'Toole, B. P. Sullivan, M. R.-M. Bruce, L. D. Margerum, R. W. Murray and T. J. Meyer, *J. Electroanal. Chem., Interfacial Electrochem.*, 1989, **259**, 217.
41 K. F. Purcell and J. C. Kotz, *Inorganic Chemistry*, W. B. Saunders, New York, 1977.
42 K. Nakamoto, *Infrared and Raman Spectra of Inorganic and Coordination Compounds*, 4th edn., Wiley Interscience, New York, 1986.
43 B. P. Sullivan and T. J. Meyer, *J. Chem. Soc., Chem. Commun.*, 1984, 1244.
44 C. R. Cabrera and H. D. Abruna, *J. Electroanal. Chem., Interfacial Electrochem.*, 1986, **209**, 101.
45 D. P. Summers, J. C. Luong and M. S. Wrighton, *J. Am. Chem. Soc.*, 1981, **103**, 5238.
46 C. Kutal, A. J. Corbin and G. Ferraudi, *Organometallics*, 1987, **6**, 553.
47 J. C. Luong, R. A. Faltynek and M. S. Wrighton, *J. Am. Chem. Soc.*, 1980, **102**, 7892.
48 P. Glyn, F. P. A. Johnson, M. W. George, A. J. Lees and J. J. Turner, *Inorg. Chem.*, 1991, **30**, 3543.
49 Y. Yamaguchi, M. Frisch, J. Gaw and H. F. Schaefer, *J. Chem. Phys.*, 1986, **84**, 2262.
50 C. F. B.-Penna, A. B. Gilchrist, A. H. K.-Oliva, A. J. L. Hanlan and D. Sutton, *Organometallics*, 1985, **4**, 478.
51 A. J. Deeming and B. L. Shaw, *J. Chem. Soc. A*, 1969, 443.
52 W. Tam, G.-Y. Lin, W.-K. Wong, W. A. Kiel, V. K. Wong and J. A. Gladysz, *J. Am. Chem. Soc.*, 1982, **104**, 151.

Received 15*th November* 1991; *Paper* 1/05801K